Georg Erharter B.Sc.

Multi Methodological Mapping and Analysis of Discontinuities as predispositional factors for Rock slope instability
Pletzachkogel / Tyrol / Austria

Master's Thesis

submitted in fulfilment of the requirements for the degree of
Master of Science

Master's Degree Program Earth Sciences

Graz University of Technology
Institute of Applied Geosciences

Supervisor
Prof. D. Scott Kieffer

Co-Supervisor
Dr. Christoph Prager

Graz, January 2018

Affidavit

I declare that I have authored this thesis independently, that I have not used other than the declared sources/resources, and that I have explicitly indicated all material which has been quoted either literally or by content from the sources used. The text document uploaded to TUGRAZonline is identical to the present master‘s thesis.

Date Signature

Acknowledgements

First of all, I'd like to thank my supervisor Prof. D. Scott Kieffer for providing all the support in terms of equipment and guidance that I needed, while simultaneously offering me the freedom for pursuing my own ideas. Special thanks go also to my co-supervisor Dr. Christoph Prager, who provided not only the initial idea of the location Pletzachkogel, but also dedicated a lot of his time and experience into me and this project. Assoc. Prof. Hugo Ortner's advice concerning the structural geology of Pletzachkogel is also appreciated.

Gerhard Lauk and Maja Bitenc are thanked for providing guidance and information in the fields of drone flying and remote sensing. The tour behind the rock buttresses and through the mountain's SE-face, guided by Thomas Außerlechner was also greatly appreciated, as it brought new perspectives and unprecedented insight to this extraordinary landscape. Eva Schwärzler and David Attlmayer, I could not have wished for any better co-pilots and porters than you guys!

Content

Abstract

The mountain Pletzachkogel (Tyrol / Austria) has been affected by major bedrock landslides (late Pleistocene, Holocene, 120-240 AD) and there is still ongoing rockfall in their steep and rugged scarp areas. The mountain is made up of a succession of Mesozoic sedimentary rocks with different lithological properties, that have been affected by synsedimentary- and tectonic deformation. Resulting from this are deep seated discontinuities that amplified processes of Quaternary post glacial stress redistribution. In combination with the presence of the incompetent Kössen Formation at the base of the mountain, overall rock mass instability and several landslides occurred.

As site access to the rockfall / scarp areas is restricted due to safety concerns, a novel approach of unmanned aerial vehicle (UAV) based photogrammetry and techniques of digital mapping is used to obtain structural geological measurements from these areas. The integration of these modern methods with classical geological field mapping yields an unprecedented quantity of structural orientation data that contribute to rock mass characterization and - analysis.

Different automatic and semi-automatic / manual methods of digital mapping are used to gather orientation data from the UAV based photogrammetric point cloud and comparisons to manual geological field measurements are made. The UAV survey's results are used to understand the overall structure of Pletzachkogel, to characterize the kinematics of the rockfall source area and to identify the basic failure mechanisms: block sliding, wedge failure and block toppling.

Future application of this workflow in different geological scenarios will show its efficiency and contribute to more objective rockmass characterization.

Zusammenfassung

Der Berg Pletzachkogel (Tirol/Österreich) ist von mehreren, massiven Bergstürzen gezeichnet (spätes Pleistozän, Holozän, 120-240AD) und bis heute treten Felssturzereignisse in den steilen Wänden auf, die die ehemaligen Abbruchkanten repräsentieren. Der Berg besteht aus einer Abfolge von Mesozoischen Sedimentgesteinen mit unterschiedlichen lithologischen Eigenschaften, welche synsedimentär und tektonisch deformiert wurden. Dadurch entstanden tiefsitzende Schwächezonen im Gebirgsverband, welche verstärkend auf die Quartäre, postglaziale Spannungsumlagerung wirkten. In Kombination mit der inkompetenten Kössen Formation an der Basis des Berges führte dies zu instabilen Gebirgsverhältnissen und mehreren Bergstürzen.

Da der Zugang zu den Felssturzgebieten aus Sicherheitsgründen stark eingeschränkt ist, wurde Drohnen-basierte Photogrammetrie und digitales Kartieren angewandt, um strukturgeologische Messungen aus diesen Bereichen zu erhalten. Diese modernen Methoden mit klassischer, geologischer Feldarbeit verbindend erhält man eine hohe Quantität an strukturellen Messungen, welche zur Gebirgscharakterisierung und Analyse beiträgt.

Es wurden verschiedene automatische, halb-automatische/ manuelle Methoden des digitalen Kartierens angewandt, um Orientierungsdaten aus der photogrammetrischen Punktewolke zu extrahieren und diese dann mit manuellen Messungen zu vergleichen. Die Ergebnisse wurden verwendet um den strukturellen Aufbau des Pletzachkogel zu verstehen, sowie um das kinematische Verhalten der Felssturzgebiete zu charakterisieren und die grundlegenden Versagensmechanismen „Block Gleiten", „Keil Gleiten" und „Block Kippen" zu identifizieren.

Zukünftige Anwendungen dieser Methodik in verschiedenen geologischen Szenarien wird ihre Effizienz zeigen und zu einer objektiveren Gebirgscharakterisierung beitragen.

Conventions

Orientations of structural features (planes etc.) are given as dip direction and dip. Small scale mass movements are considered to have a volume of up to 1000m³.

1. Introduction

Pletzachkogel is a mountain in the Austrian province of Tyrol (Figure 2-1) that was the site of major landslides in the past and some of its steep rugged cliffs still exhibit rockfall activity that damages local infrastructure. Patzelt (2012) investigated the depositional age of the major landslides, but so far, no studies regarded geological factors for the morphology of the mountain, landslides or the rockfall events. The geological structure of Pletzachkogel has only been mentioned in few other studies (e.g. (Ampferer, 1908; Resch *et al.*, 1986)) and the mountain has been given as an example in context of landslides (Prager *et al.* 2008; Huttenlau and Ortner-Brandstötter 2011).

The goals of this study are to: (1) use and evaluate a novel approach of Unmanned Aerial Vehicle (UAV) based photogrammetry with methods of digital mapping for joint set identification; (2) identifying factors that led to the landslides and influenced the morphology of Pletzachkogel.

Assessment of rock fall hazards in steep mountainous terrain is often encumbered by personnel access constraints and safety concerns. Photogrammetry based on Unmanned Aerial Vehicle (UAV) data collection platforms greatly enhance observational access to restricted terrain, while also providing 3D georeferenced point clouds of sufficient resolution and accuracy to permit reliable digital structural geologic measurements. The efficacy of deploying small, portable UAVs in the context of rockfall source area analyses is evaluated. This evaluation is based on comparing point cloud derived, digital discontinuity orientation measurements to structural measurements made in the field with a geologic compass. Methods for extracting the structural measurements from the point cloud included manual/interactive techniques as well as semi-automated and automated discontinuity detection algorithms. Classical engineering geological and geomorphological mapping is done for understanding the mountain's architecture. The results from the traditional field survey and the UAV based mapping are combined to interpret the observed phenomena.

In chapter 2, an overview of the area is given and for orientational purpose some geographical locations are described that will be referred to later. Chapter 3 presents the stratigraphic and tectonic setting of the mountain and in chapter 4 the used methodology is elaborated. In chapter 5 the results of the UAV survey and the field mapping are presented. The results are interpreted in chapter 6 and final conclusions are drawn in chapter 7.

2. Geography and historic landslides

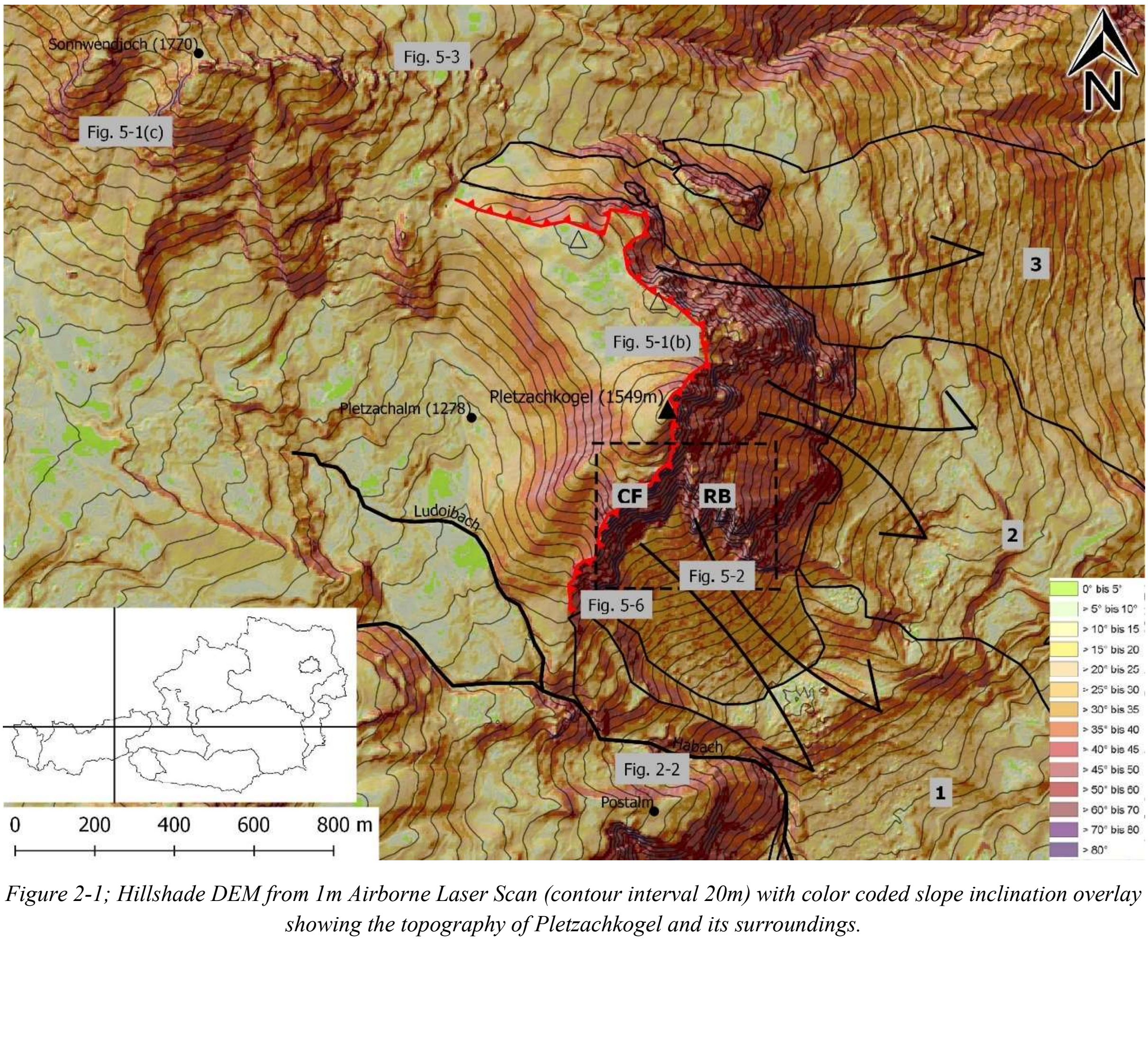

Figure 2-1; Hillshade DEM from 1m Airborne Laser Scan (contour interval 20m) with color coded slope inclination overlay showing the topography of Pletzachkogel and its surroundings.

Landslide crowns and deposits are marked 1 = last- (120-240AD), 2 = middle Holocene- and 3 = late Pleistocene - landslides (Patzelt, 2012). Dashed rectangle at Pletzachkogel SE-cliff face (CF) and rock buttress area (RB) indicates UAV-surveyed scarp area. Geographical locations and positions of figures are given for orientational purposes (tiris, 2017).

Pletzachkogel is located in Tyrol (Austria) and has a peak elevation of 1549 m a.s.l. With 1770m a.s.l. the next higher elevation is Sonnwendjoch which is separated from Pletzachkogel's summit by a col, NE of the mountain. The following locations are shown in Figure 2-1 and will be referred to later in the text: Ludoibach and Habach are the only named creeks in the study area and are located SW-S of the summit; Postalm, a hut S of Habach; Pletzachalm, a hut W of the summit.

Topographically, Pletzachkogel is dominated by a near vertical and southeast facing cliff having a relief of >250m. On its southeast side Pletzachkogel is bordered by a series of prominent vertical rock towers that are up to 200m high and are referred to as the "rock buttress" (Figure 2-1 & Figure 2-2). As depicted in Figure 2-1, three major Holocene landslides have sculpted the morphology of the mountain (Patzelt, 2012). The oldest, dated landslide was a late Pleistocene event with an age of around 12500 ± 400 BC on the NE side of Pletzachkogel ((3) in Figure 2-1). Following this was a series of Middle Holocene landslides between 2000 and 1700 BC, originating from the E side ((2) in Figure 2-1). The cliff and rock buttress on the SE side of the mountain represent the head scarps of a major landslide that occurred at around 120-240 AD (Patzelt, 2012) ((1) in Figure 2-1). The dating has been done by means of radiocarbon dating. The full extent of the landslide deposits is shown in the minimap on the geological map (Appendix 3). As can be seen there, all the landslides crossed either the rivers "Brandenberger Ache" to the East or the river "Inn" to the South and blocked their respective valleys.

Because of erosion from these rivers and anthropogenic activity in the Inn-valley, only vague estimations about the volume of the landslides can be made. Patzelt (2012) estimates a total volume of all landslide deposits of up to $93x10^6$ m³, the majority thereof (approx. $50x10^6$ m³) belonging to the 120-240 AD event.

Subsequent to these landslide events, rockfalls have represented an ongoing geologic process in the headscarp region. The most recent significant rockfalls occurred in 2011 and 2015 and their source areas can be recognized by its light color in Figure 2-2 (ORF, 2015). Debris volumes of these events exceeded 1000m³ and the rockfall threatened paths and roads below the cliff. The rockfall source areas are located above a 300m high talus fan, featuring site access constraints due to potential rockfall hazards.

Figure 2-2; The southeastern cliff face of the Pletzachkogel (left) and the rock buttress (right). The source areas and deposits of the 2011 (left arrow) and 2015 (right arrow) rock falls are indicated by freshly exposed rocks in the buttress area. Note major joints shaping the rock mass.

3. Stratigraphic and tectonic setting

Pletzachkogel is located at the southern margin of the Northern Calcareous Alps (NCA). The NCA are an E-W striking mountain range, comprised of non- to weakly metamorphic (Frey *et al.*, 1999) Mesozoic sediments, that have undergone NW directed, thin skinned thrusting during Alpine orogenesis and represent allochthon rock units, tens of kilometers away from their origin (Schmid *et al.*, 2004) (see Figure 3-1). The first stage of Alpine orogenesis led to internal deformation and nappe stacking of the NCA. The area of Pletzachkogel is characterized by NW-SE trending, transverse high angle faults and NW-directed low- and high angle fold - thrust faults (Eisbacher and Brandner, 1995). To the South, Pletzachkogel is bordered by the Inntal-shear zone which is a major sinistral strike-slip fault, resulting from eastward extrusion of crustal wedges during the second stage of Alpine orogenesis (Ortner *et al.*, 2006).

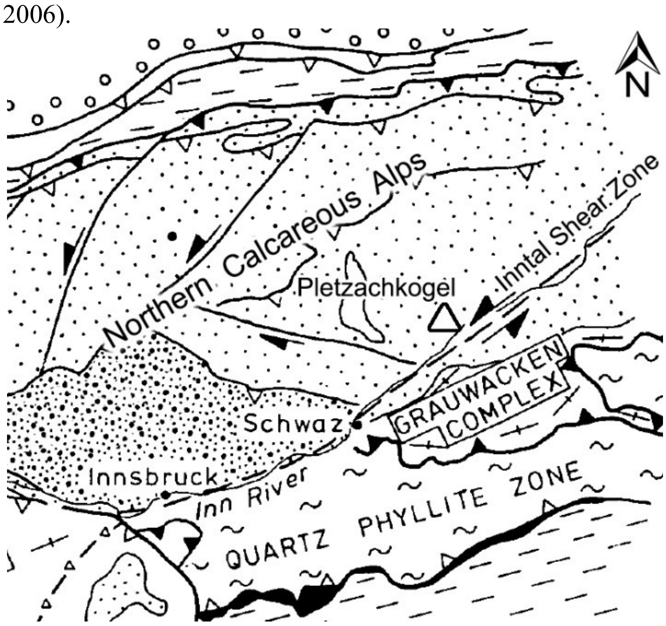

Figure 3-1; Geological overview map of Pletzachkogel (hollow triangle) and its surroundings; (Eisbacher and Brandner 1995, modified).

The lithological setting of the Pletzachkogel area is characterized by various upper Triassic to lower Jurassic sedimentary rocks. The stratigraphically lowest unit is the Hauptdolomit (HD) which comprises mainly well bedded dolostones. The HD succession (Norian) is of shallow marine origin with thicknesses of up to 2000m (e.g. Fruth and Scherreiks (1982); Donofrio *et al.* (2003)). Next higher unit is U-Norian "Plattenkalk" (PK). With well bedded, varying successions of dolostones, limestones and intercalated marls/claystones in the lower part and dominant limestone bedding in the upper part, it represents a deeper marine origin than HD. Towards the top, first appearance of meter-thick marls and bioturbated/fossiliferous limestones represents the transition to the next higher Kössen formation (Czurda, 1970). The U-Norian to Rhaetian Kössen Formation (KFm) consists of well-stratified alternations of marls and limestones. (Holstein, 2004; Piller *et al.*, 2004).

Lying atop of the KFm and representing the uppermost Triassic unit is the "Oberrhätkalk" or "Steinplattenkalk" (ORK). The origin of this thick bedded to massive limestone unit is a shallow marine reef complex interfingering with the Kössen basin beds (Flügel and Stanton, 1989). The rock mass forming Pletzachkogel's slopes and summit is comprised of lower Jurassic breccia (Resch *et al.*, 1986). It is a, reddish to grey, obscurely stratified to massive breccia with components consisting of dolomite and limestone, some fossiliferous. In some parts, the rock consists exclusively of crinoids. The highly variable stratigraphy makes an assignment to different stratigraphic units difficult. Similarities to the "Hierlatzkalk" are present but also features of "Schafkopfschichten" can be found (Ortner, 2017). According to Vörös (1991), Hierlatzkalk is originating from localities close to submarine fault zones and taluses. The key point is that the unit has undergone synsedimentary deformation that has possibly also affected the below lying ORK and created potential zones of weakness even prior to the alpine orogenesis.

The stratigraphic succession is discordantly overlain by clastic Gosau sediments (U-Cretaceous to L-Eocene; Ampferer 1908; (Wagreich and Faupl, 1994) which are exposed West of Pletzachalm. The bedrock units in the Pletzachkogel area are widely covered with various quaternary sediments. These include glacial till, deposits of three major landslides (Patzelt, 2012) and talus deposits.

4. Methodology

4.1 Geological Mapping

In order to assess the rock mass structure of Pletzachkogel and the landslides, the landslide sources and surrounding areas were geologically mapped at a scale of 1:5000 (see geological map in Appendix 3). Mapping focused on geology, morphological features of mass movements, discontinuity characteristics (orientations) and hydrology (springs, creeks, marshland). Further morphological and structural mapping was performed by GIS-based analyses of hillshade digital elevation models of the 1m airborne laser scan (ALS) provided by tiris (2017). Deposits of the major Holocene landslides were modified after Patzelt (2012), with main changes concerning the extent of the late Pleistocene landslide deposits near the head scarp area.

4.2 UAV photogrammetric survey and image processing

Aerial photographs were acquired with the DJI Mavic Pro ("Mavic") quadrocopter. The Mavic is well suited to alpine environments by virtue of its compactness, flight duration and photographic capabilities. Technical specifications of the Mavic are summarized in Table 1. With a standard GPS accuracy of >5m, the Mavic's on-board GPS system is not sufficiently accurate for direct georeferencing of the photogrammetric point cloud, requiring indirect georeferencing with precisely surveyed ground control points (GCPs). The used GCPs are specially fabricated optical targets for the use in alpine environments (Figure 4-1), whose center coordinate can be identified and precisely selected directly on overlapping aerial photographs.

Table 1; DJI Mavic Pro key technical specifications (DJI, 2017)

UAV	Weight [g]	734
	Size (folded) [mm]	83 x 83 x 198
	Max. flight time [min]	27
camera	Sensor type	CMOS
	Sensor format	1/2.3
	Sensor dimensions [pixels]	4000 x 3000
	Sensor dimensions [mm]	6.2 x 4.6
	Image resolution [Mpixels]	12.35
	Focal length [mm]	28
	ISO	100-1600

Figure 4-1; GCP specially fabricated for use in alpine terrain

In consideration of model size and computational effort, the UAV survey area was spatially divided into three "chunks". Chunk 1 and 2 include the buttress towers, and chunk 3 comprises the SE-facing main cliff. Six GCPs were established for each chunk (their coordinates can be found in Appendix 1). In Figure 4-2, the division of the survey area into chunks and the position of the GCPs is given. Due to a multitude of topographic obstructions and flight hazards, UAV photograph acquisition was performed in a manual flight mode rather than autonomously (pre-programmed flight plan). The pictures of chunk 1 and chunk 2 were taken on the 21st of May 2017 and the pictures for chunk3 on the 28th of June 2017. On the first flight day, the weather was mostly sunny with singular clouds and strong, uphill directed winds. The weather on the second flying day was a mixture of clouds, fog and phases of heavy rain on the forenoon, but a change towards strong sun permitted flying in the afternoon.

In total 853, 779, and 1931 overlapping photographs were acquired for chunks 1, 2, and 3, respectively. The raw photographs were manually sorted (e.g. blurry, heavily over- or underexposed, or redundant images were removed from the data set) and georeferenced point clouds were then generated applying the software *Agisoft PhotoScan Professional* (Agisoft, 2017). Settings for point cloud generation and properties of the point clouds is given in Appendix 2. Figure 4-3 (a) and (b) shows a comparison of an original UAV image to the final dense point cloud.

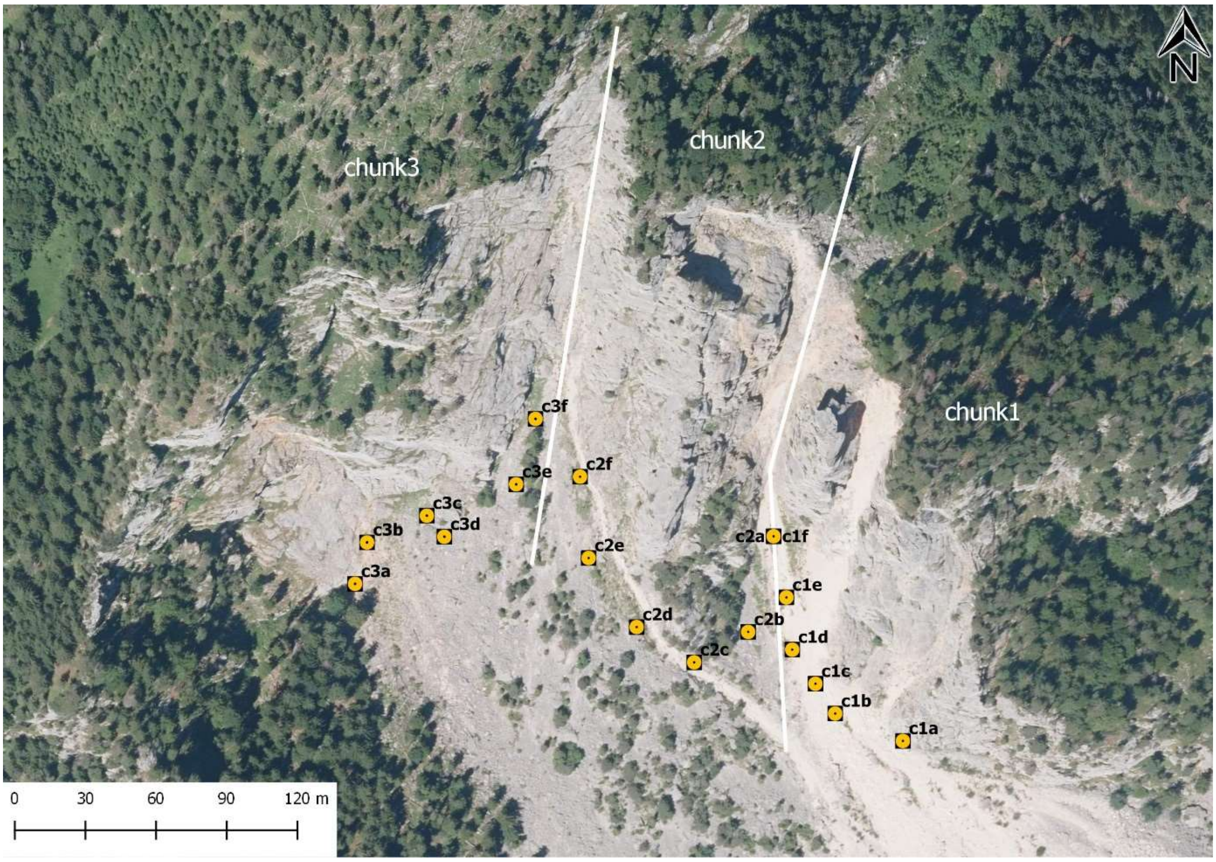

Figure 4-2; Orthophoto of the UAV survey area. The buttress area was divided into chunk 1 & -2, chunk 3 is comprised of the SE- cliff face. The GCPs are marked and labelled corresponding to the table of Appendix 1.

4.3 Digital mapping and kinematic analysis

Two plugins for the open source 3D point cloud processing software *CloudCompare* (CC) (version 2.9. beta) were used to extract plane orientations (CloudCompare, 2017): *Facets* and *Compass*.

Facets is a CC plugin for fully automatic structural data extraction (Dewez *et al.*, 2016), which divides the point cloud into clusters of adjacent points and employs a least square plane fitting algorithm (Figure 4-3 (d)). Following user defined criteria of co-planarity, the clusters are reassembled in a three-step process: (1) elementary facets corresponding to small fragments of planes are computed; (2) elementary planes are then re-clustered into encompassing planes; and (3) parallel planes are merged into plane families. The end result is a number of polygons that are color coded according to their spatial orientation (azimuth/dip). The data can be exported as .csv or .shp files, or analyzed directly in CC (Dewez *et al.*, 2016). The user defined input parameters selected for the *Facets* analysis are summarized in Table 2.

Table 2; Input parameters for the Facets "fast marching approach."

Octree level	10
use retro projection error for propagation	yes
Max distance @99%	0.213
Min points per facet	3500
Max edge length	0.7

Compass is an additional CC plugin for extracting and exporting manual or semi-automated structural measurements from point clouds using a plane-, trace- and lineation- measurement tool (Thiele et al., 2017) (Figure 4-3 (c)). Using a least square algorithm, Compass fits a plane to a group of sampled points. Selection of points is facilitated by an adjustable sampling-circle around the cursor. The plane-tool is applicable to exposed surfaces, while the trace-tool can extract orientation based on the geometry of a discontinuity edge intersecting an irregular outcrop surface. The start and end points of a discontinuity trace are specified, and the tool finds the linking "structural trace" using a "least cost path" algorithm. A planar surface is then fitted to each trace with a least square algorithm to obtain an "estimate of the structure orientation". The lineation-tool simply measures the trend and plunge of a straight line between two points.

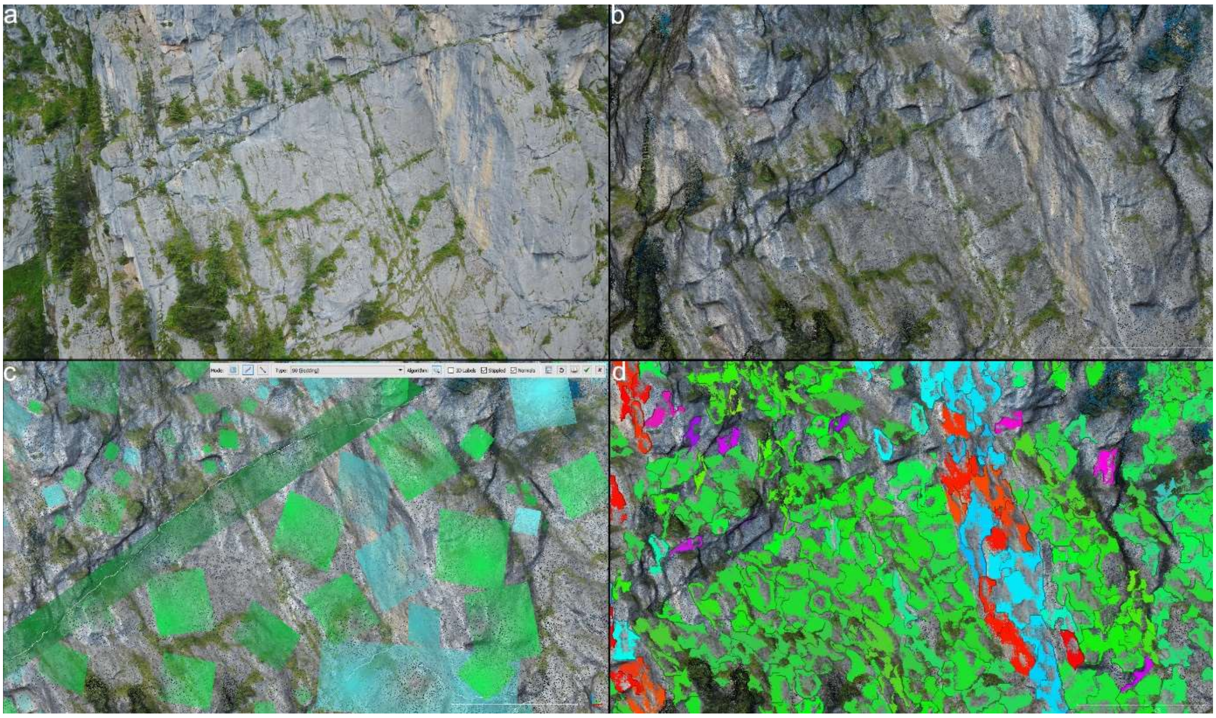

Figure 4-3; (a) original UAV image of a part of the SE-cliff face; (b) respective part of the dense point cloud; (c) manual and semi-automatic plane measurement with CC-Compass; (d) automatic plane extraction with CC-Facets.

On the basis of UAV derived structural measurements (orientations of discontinuities), simple kinematic analyses were performed to obtain an initial estimate of block failure mode tendencies. The main focus of the kinematic analyses included the Pletzachkogel southeastern cliff face and neighboring rock buttress area. The kinematic conditions for planar sliding, wedge sliding and toppling were evaluated (e.g. (Wyllie et al., 2004)).

5. Investigation Findings

5.1 Geomorphology

Pletzachkogel is characterized by a hummocky summit "plateau" with one main summit and two lower high points to the North, separated by linear depressions. While the western slope of the mountain shows an inclination between 20° - 45°, the N-, E- and S- sides are steep slopes with >50°. A multitude of plate-like and columnar rock bodies with sizes up to several tens of meters can be found at the N-, E- and S slopes' foot. Talus fans originate from the foot of these slopes and steep rock cliffs are protruding from the ground and extend for hundreds of meters. On the talus fans and the rock slopes, deposits of the 2011-, 2015- and more recent rockfall events can clearly be differentiated from older deposits by their light red to orange color, compared to the dark grey, weathered older deposits.

37 cracks, crevasses and linear depressions on the summit area were mapped in the field and on the ALS data and are shown in the geological map (Appendix 3). The majority of the cracks is located close to the southeastern cliff (120-240 AD landslide scarp), is orientated subparallel to it (i.e.: strike: NE-SW) (CS1 in Figure 5-1 (a)), and is showing apertures of ca. 10-50cm. Another set of crevasses can be found north of the main summit and strikes NW-SE (~165°) (CS2 in Figure 5-1(a)). Parallel to this set of cracks, several depressions can be found on the summit plateau and parallel to the NE face, showing lengths up to at least 70m, and depths and apertures of ca. 5m. The biggest crevasse with a measurable length of 87m, an aperture of up to 5m (at ground surface) and a visible depth of at least 30m strikes also NW-SE and is located on the western side of the first high point north of the main summit (Figure 5-1 (b)).

The slope between Sonnwendjoch and the col, NW of Pletzachkogel, has an inclination of around 30-35°. The northern and western edge of this slope is characterized by 10-20m high vertical cliffs with gentle grass-slopes bordering directly onto them (Figure 5-1(c)). Rock blocks with a diameter of up to 40m are lying on the grass-slopes near the edge of the cliffs and on flat spots downslope.

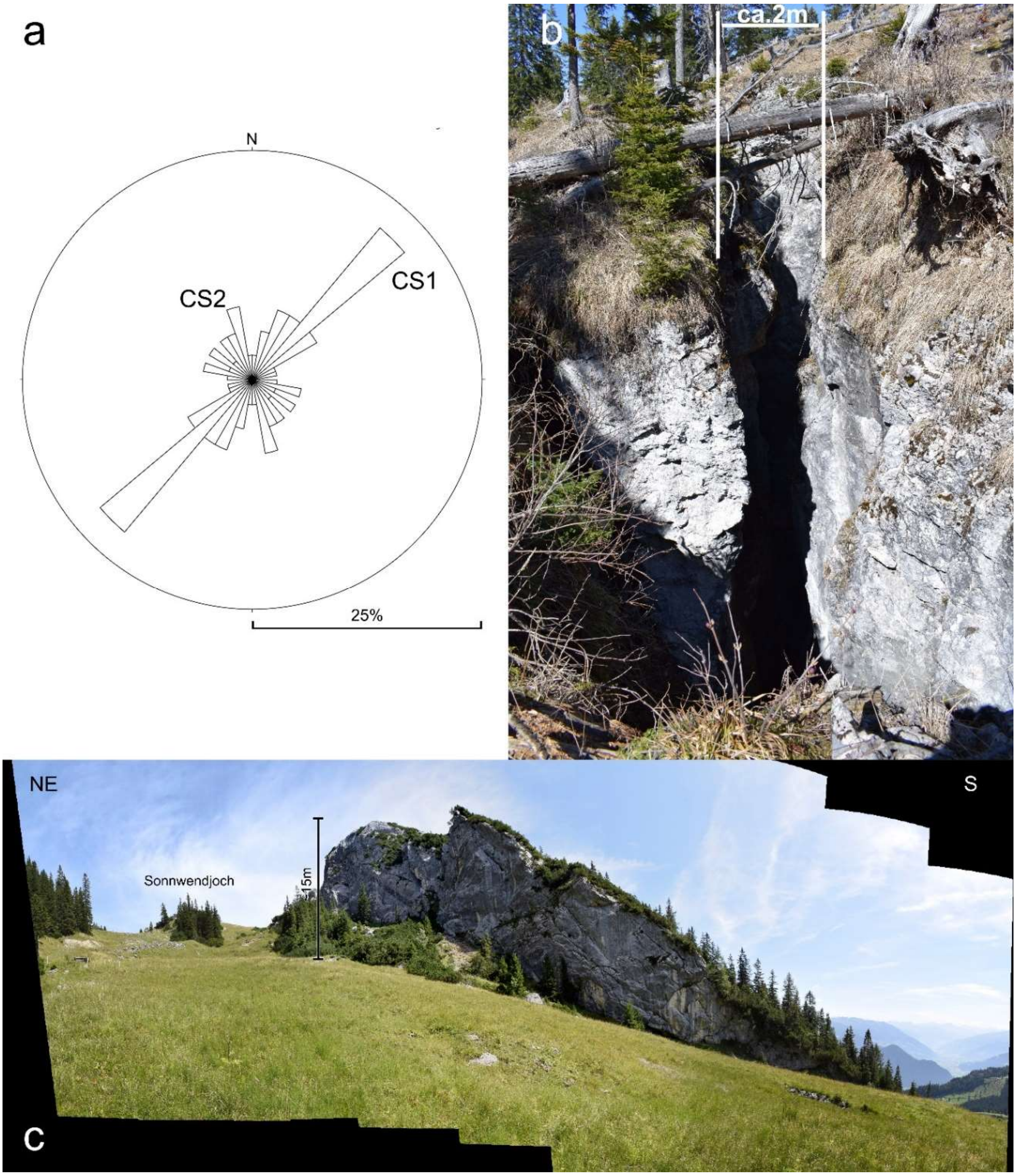

Figure 5-1; Morphological features of Pletzachkogel: (a) Rose diagram of depressions, cracks and crevasses at the summit plateau of Pletzachkogel. Radial scale is given as % of total amount.; (b) The largest exposed crevasse at the summit area of Pletzachkogel; (c) The cliffs that confine the rock slope between Pletzachkogel and Sonnwendjoch.

5.2 Lithologic Units

Hauptdolomit (HD) is a fine crystalline (microsparite), light beige - light grey colored dolomite, generally well stratified with 10-100cm thick bedding planes. It shows a high weathering resistance with only superficially discolored surfaces. Gradually transitioning from dolomite to limestone, the next higher unit is the well bedded, fine grained limestone - "Plattenkalk" (PK). Compared to HD its surface is discolored and shows karstic dissolution phenomena. Karst in this unit is undeveloped (k1), following the classification of (Waltham, 2002). Small outcrops of PK can be found in the meadows around "Postalm" South of Pletzachkogel, but its main occurrence is North and West of Sonnwendjoch.

The Kössen Formation (KFm) is a weak unit of alternating layers of limestone and marl that is prone to erosion (Figure 5-2). An unconfined compressive strength (UCS) of max. 25MPa can be estimated for limestone layers and a maximum of 5MPa for marls (based on field estimations acc. to ÖN 14689-1). KFm creates distinctively gentle landforms. This morphology can best be seen at the slope between Sonnwendjoch and the col NW of Pletzachkogel which consist of the hard Oberrhätkalk and is encircled by KFm, thereby creating the rugged cliff-morphology (see Figure 5-1 (c)).

Oberrhätkalk is composed of grey to light beige (fresh; weathered dark grey), fine – medium grained limestones, obscurely stratified to massive. Except some few outcrops, hardly any bedding can be observed. Discolored surfaces and only minor signs of karstic dissolution are present. Rock UCS is estimated being around 100-150 MPa. In the study area, Oberrhätkalk is encountered along the basis of Pletzachkogel's rock cliff faces and the slope between Pletzachalm to Sonnwendjoch.

The transition from ORK to the overlying lower Jurassic breccia (LJB) is gradual, i.e. comprising a zone some tens of meters thick where the rock's color changes from light beige to brick red. The facies varies locally, from a fossil bearing breccia (with limestone and dolomite components up to 10 cm in a brick-red or white, fine calcitic matrix) to medium coarse, brick red rocks consisting completely of crystallized crinoids with a sugary fabric (Figure 5-3). The breccia is diagenetically well cemented, with rock/rock mass strength and weathering properties similar to the ORK. Joints are partially filled with very fine grained, dark red-brown clayey sediment. The main rock mass of Pletzachkogel consists of LJB and outcrops can also be found south of Habach.

Outcrops of Gosau occur west and south of Pletzachalm, showing incompetent facies varying from grain supported sandstone to coal and fossil bearing breccia.

Figure 5-2; one of the few Kössen Formation outcrops.

Figure 5-3; Lower Jurassic Breccia makes up most of Pletzachkogel's main body

Unit thickness of HD and LJB could not be determined since the lithostratigraphic base, respectively cover is not exposed in the study area. A thickness of 125m is inferred for ORK and 85m for KFm. However, these values are varying in reality due to inhomogeneous sedimentation and synsedimentary deformation. Three main mechanical units can be differentiated: i) the rigid foundation of the mountain, consisting of strong HD and PK; ii) KFm as weak and incompetent unit; iii) ORK and the LJB as strong, brittle cover.

5.3 UAV survey

For chunk 1 a dense point cloud (DPC) consisting of 41,805,462 points was generated with a ground resolution of 3.04cm/pixel and a reprojection error of 1.11 pixel. The DPC for chunk 2 consists of 49,762,919 points with a ground resolution of 2.3cm/pixel and a reprojection error of 1.23 pixel. For chunk 3, the DPC consists of 42,481,210 points with a ground resolution of 3.42cm/pixel and a reprojection error of 1.68 pixel. In the areas of primary interest (i.e. bedrock outcrops), the image overlap is greater than nine.

With the CC plugin *Compass*, 1394 structural measurements were extracted, and with the plugin *Facets*, 5238 planes were extracted. As shown in Figure 5-4, there are two main orientation clusters. For the *Compass* measurements, the cluster centers have a dip direction/dip of 127/68 and 183/88, and for the *Facets* measurements, the corresponding center orientations are nearly identical at 124/69 and 180/86.

The joint set orientations determined on the basis of point cloud- and manual field measurements are summarized in Table 3. As indicated therein, the point cloud derived measurements underrepresent a third discontinuity set having an orientation of approximately 280/60. The underrepresentation of this joint set is related to the characteristically small surface areas of joint faces exposed in the outcrops.

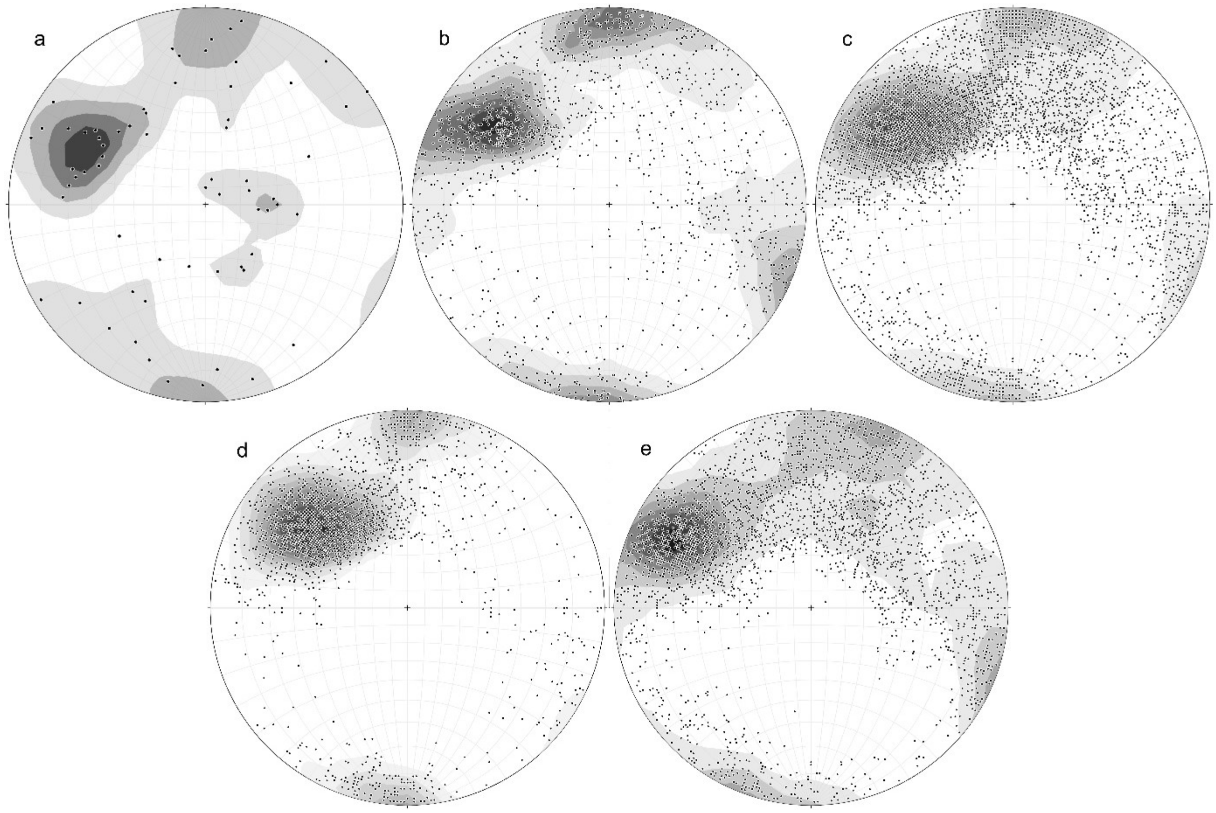

Figure 5-4; equal angle, lower hemisphere, stereographic projections: (a) due to safety reasons, not more than 67 manual measurements could have been taken from the area at the foot of the SE-cliff face and the rock buttress; (b) 1394 poles of manual and semi automatically extracted planes from the survey area with ccCompass; (c) 5238 poles of automatically extracted planes of the survey area with ccFacets; (d) portion of the poles from ccFacets that belong to the SE-cliff face; (e) portion of the poles from ccFacets that belong to the rock buttress area.

Discontinuity set orientations measured for the rock buttress are similar, but scattering of the results is more significant than for the southeastern cliff face. The underrepresented third joint set, having an orientation of 270/70, was also detected in the point cloud for the rock buttress.

Table 3; Average joint set orientations obtained from photogrammetric point clouds (SE-facing main cliff (Figure 5-4 (d))and rock buttress area (Figure 5-4(e))), and from manual field measurements (Figure 5-4(a)) in the investigated area.

	southeastern cliff face	**rock buttress**	**field measurements**
joint set 1	129/64	116/75	103/65
joint set 2	181/88	202/87	190/80
joint set 3	280/60	270/70	270/35

5.4 Structural Geology

The cross sections presented in Appendix 4 show the tectonostratigraphic setting of the project area (top row of cross sections), an interpretation of the present surface geology (bottom row of cross sections) and the inferred situation before the landslides occurred (middle row of cross sections).

The cross sections show that the outcrop pattern of KFm correlates on all sides with a morphological break from flat to steep. Whereas the gently inclined area at the foot of the slope break is comprised of PK and HD, the steep slope sections above are comprised of ORK and LJB.

5.4.1 Folds

The overall geological structure of the mountain is characterized by an asymmetric, NNW verging syncline with a gently dipping N-limb (backlimb) and a recumbent S-limb (forelimb) (henceforth termed “Pletzachkogel Syncline”). The backlimb is defined by a moderately steep (30-45°) SSE dipping slope of PK, KFm and ORK between Sonnwendjoch and areas south of the main summit. The forelimb is composed of steeply N-dipping and sub vertical oriented units of HD and PK, located South of Habach and around Postalm. The poles of the measured bedding planes are given in Figure 5-5 and show the large fold structure. Due to the massy structure of ORK and the LJB, only few secondary folds are encountered. Some of them were detected by UAV on top of the rock buttress area and are parallel to the big Pletzachkogel Syncline.

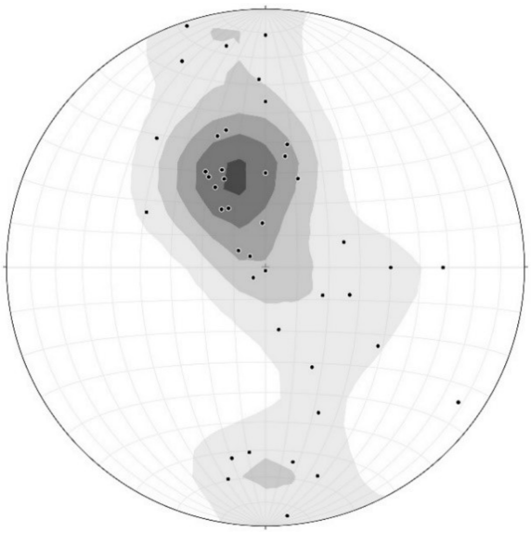

Figure 5-5; manually measured orientations of bedding planes at Pletzachkogel (contoured pole plot, equal area, lower hemisphere, stereographic projection) Poles of SSE dipping planes (i.e. N-limb of the syncline) are quantitatively dominating because covering larger areas of the study site (compared to the poles of N-dipping planes, i.e. S-limb of syncline).

5.4.2 Faults

Two different orientations of faults or fault zones have been observed at Pletzachkogel: (i) a sub horizontal fault at the foot of the SE cliff face; (ii) a fault set which is subparallel to joint set 1 from Table 3.

(i) A distinct fault zone is exposed at the southern foot of Pletzachkogel's SE face (Figure 5-6): at least 2m thick, intensively sheared, red to grey limestones (LJB) and fault breccias are exposed. The fault zone orientation is slightly undulating with comprising gently NNW- dipping fault planes (#4 in Table 4 & Figure 5-7). Fault kinematics are unclear, since unambiguous shear sense indicators have not been observed yet. However, this fault is considered relevant for rock slope stability in view of mechanical parameter (weakness zone, reduced rock mass strength) and hydrogeological characteristics (hydraulic permeability inferred being lower than those of the overlying fractured ORK/LJB, i.e. aquitard). Its parallel orientation to the below lying KFm is making it to yet another weak layer in the rockmass with the potential to influence above lying, brittle rock units.

Figure 5-6; distinct fault (weakness zone) at the southern foot of Pletzachkogel's SE cliff face, featuring intensively sheared, red to grey limestones (HK). Fault zone is slightly undulating, comprising gently NNW- and SSE-dipping planes (see Table 4: #5). Exposed fault thickness > 2m.

(ii) The following faults are all considered to belong to one set of faults which will be termed “Fault set 1” in Table 4 and afterwards. Several faults within ORK and LJB are steeply dipping SE and indicate sinistral shear sense based on slickenfibre orientations. One of these faults, north of Pletzachalm, can be connected to the morphological depression that forms the col north of Pletzachkogel. The exact assignment of this morphological feature to tectonics or gravitational movement is unclear.

A reverse-fault, parallel to the fold axis plane of the Pletzachkogel syncline is inferred for the following reasons: tight folding as such cannot occur without faults, while simultaneously maintaining the units’ layer-thickness; faults and intense scattering of bedding orientations have been observed in the proximity of the syncline’s core at the HD outcrops in the eastern project area; the orientation change from ca. 160/20 to 340/75 occurs within tens of meters which is hardly possible without any brittle deformation; fold axis plane parallel thrust- or reverse faults are well known from other locations in the NCA.

At the top of Sonnwendjoch, a cliff of ORK is rising out of the KFm and is bordering directly onto PK. This is seen as the expression of a bedding – parallel thrust fault which results in doubling of the stratigraphic succession and has an orientation of about 150/40.

The area South of Habach, where LJB was mapped, is very close to the core of the Pletzachkogel syncline. The morphological depression and lack of bedrock outcrops directly South of it is interpreted as the expression of the KFm (like at Sonnwendjoch) that overlies PK which crops out further South. The absence of ORK between KFm and the LJB can either be explained with yet another fault connected to the Pletzachkogel syncline or simply a stratigraphic feature of the interfingering facies.

5.4.3 Summary of Discontinuities

In Table 4 and Figure 5-7 the identified main sets of discontinuities are given. Joint sets 1-3 were measured by UAV. Fault #4 is the sub-horizontal fault that was observed at the base of Pletzachkogel and #1 the set of faults that was described in the end of the previous chapter.

The sliding directions of the landslides identified by Patzelt (2012) are estimated as ENE (60°) for the late Pleistocene-, ESE (120°) for the mid-Holocene- and S (180°) for the 120-240 AD landslide and are also given in Figure 5-7.

*Table 4; Main discontinuity sets observed at Pletzachkogel. * = UAV measurement*

Discontinuity sets	orientation
#1 (faults/ joints)*	130/70
#2 (joints)*	180/88
#3 (joints)*	275/65
#4 (fault)	350/10

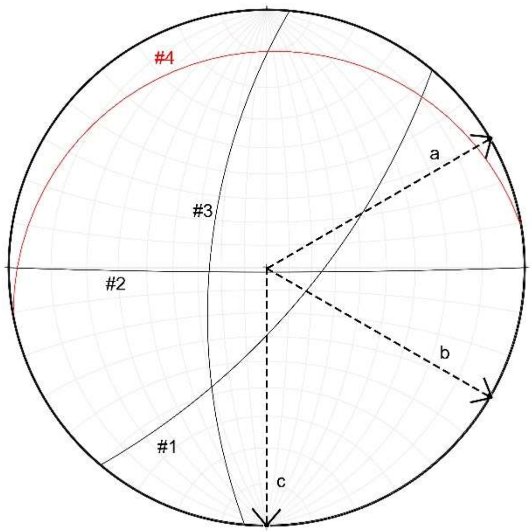

Figure 5-7; Main discontinuity sets #1-4 from Table 4 displayed in a lower hemisphere, equal angle stereographic projection. The dashed arrows indicated the approximate sliding directions of the (a) late Pleistocene, (b) mid-Holocene and (c) 120-240 AD landslides.

6. Interpretation

6.1 Small scale failures - SE cliff face

Data from the UAV survey and digital mapping were not only used for identification of the mountain's main joint sets, but also for a kinematic analysis of the failure modes present in the SE-cliff face and the rock buttress area. In the simple kinematic analyses, the entire populations of structural measurements derived from the DPCs were utilized as input and separated into the measurements from the southeastern cliff face and from the rock buttress. The southeastern cliff face orientation was taken at 140/70, and kinematic analyses for the rock buttress area explicitly considered the near-vertical columnar geometry of the rock towers by introducing a composite convex free-space formed by the intersection of slope orientations: 110/75, 200/75, and 290/75. The analysis results for the southeastern cliff are shown in Figure 6-1. A mean joint friction angle of 35° was estimated, in view of discontinuity properties observed in the field (Barton, 1976)). The analyses indicate that planar sliding is kinematically permissible along Joint Set 1, as is wedge sliding along the intersection lines of Joint Sets 1 and 2. Comparatively few structural elements of the SE cliff are susceptible to toppling failure. However, the steeper, S - to SSW-facing parts of the wall may be more prone to toppling failure (e.g. S, see Figure 6-1(a)).

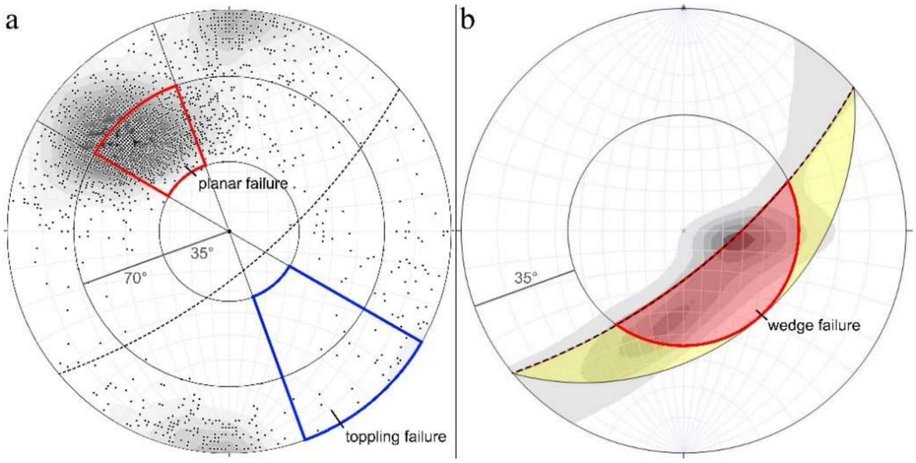

Figure 6-1; Kinematic analysis of southeastern cliff (equal angle, lower hemisphere stereographic projection of discontinuity poles): (a) structural elements susceptible to planar and toppling failure (inner circle: friction angle = 35°; intermediate circle: slope angle = 70°); and (b) density contour plot of 2,413,850 joint intersection lines, with red shaded domain indicating structural elements susceptible to wedge failure (inner circle: friction angle = 35°). Free slope surface is indicated as dashed great circle.

6.2 Small scale failures – Rock Buttress

Analysis results for the rock buttress area are summarized in Figure 6-2. As shown, planar and toppling failure are kinematically permissible along every side of the rock towers, excluding the not free northern side. Due to the increased scattering of joint orientations at the rock buttress, the analyzed joint intersections produce a wide range of intersection lines meeting the kinematic requirements for wedge failure, notably along intersection lines plunging toward the south. The increased data scattering is possibly related to the near-vertical columnar structure of the rock towers, providing an opportune geometry for long-term relaxation of the rock mass in the absence of lateral stresses.

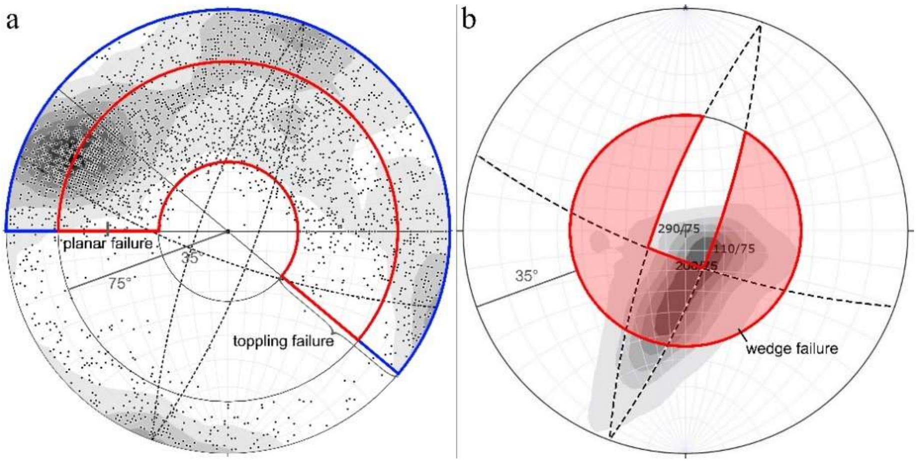

Figure 6-2; Kinematic analysis of rock buttress area (equal angle, lower hemisphere stereographic projection of discontinuity poles): (a) structural elements susceptible to planar and toppling failure (inner circle: friction angle = 35°; intermediate circle: slope angle = 75°); and (b) density contour plot of 4,618,676 joint intersection lines, with red shaded domain indicating structural elements susceptible to wedge failure (inner circle: friction angle = 35°). Free slope surfaces are indicated as dashed great circles.

6.3 Influences on Slope Stability

Two of the observations are seen as major predisposition factors for landslides at Pletzachkogel:

1. low angle, soft layers (Kössen Formation and fault) positioned below hard rock units at the base of the landslide-affected rock mass.
2. high angle, deep seated, tectonically induced brittle fracture zones encountered within the landslide-affected rock mass.

The interaction of these factors with Quaternary, post glacial processes of stress redistribution has led to the major landslides and shall be discussed below.

Ampferer (1908) mentioned that KFm is the reason for the landslides at Pletzachkogel, but without further evidence. The destabilizing effect of KFm towards overlying units is exemplified on a small scale by the behavior of the platform of ORK between Sonnwendjoch and Pletzachalm. While ORK is relatively resistant against weathering and erosion, the below lying KFm is highly affected by it. Continuous erosion of the foundation of ORK creates the characteristic steep and partly overhanging cliffs at the limestone-platform's rim (Figure 5-1(c)). Breakoff of blocks with sizes up to 1000m³ is induced, when erosion exceeds a limit and the limestone can no longer support its own weight over the weak foundation. Big blocks of broken off ORK can be found at the rim of the platform or at flat spots downhill after rolling there. A schematic representation of this process of foundation erosion is given in Figure 6-3.

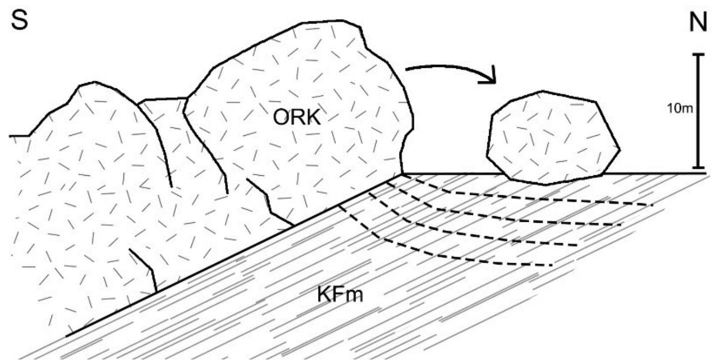

Figure 6-3; Progressive erosion affects well-bedded, weak Kössen Formation (KFm) and destabilizes jointed Oberrhätkalk (ORK).

On a big scale, the whole shape of Pletzachkogel is seen as the result of the destabilizing effect of KFm. Due to the inherently weak nature of KFm, the massif, rigid limestone cover above it (i.e. ORK & LJB) has no stable foundation and is breaking apart driven by gravity. This peculiar geomechanical system is traditionally termed "Hart auf Weich" – hard on soft – and is known from other locations in the Alps where similar stratigraphic conditions are at hand (Poisel and Eppensteiner, 1988, 1989). E.g. Eibsee rock avalanche detached from Zugspitze massif (Golas, 1996; Prager *et al.*, 2008).

Poisel and Eppensteiner (1988) showed that within a homogeneous, circular, rigid plate that overlies a soft base, concentrated, horizontal tensional stresses develop at the rim of the plate and lead to three sets of discontinuities: a set of tension cracks parallel to the rim; a set of tension cracks developing radially from the center of the plate; a set of normal fault style - shear fracturs at the rim of the plate, dipping into its body. "In any case will the rim of the hard plate be fragmented into plate like, respectively columnar joint bodies.". However, they pointed out that if there are already preexisting sets of sub-vertical discontinuities, these will be reactivated and opened by the mechanism and only subordinated, new cracks will develop. Therefore, the clear separation of structural features into ones caused by tectonics and ones caused by rock slope deformation is hardly possible (Poisel and Eppensteiner, 1988).

The depressions, cracks and crevasses in the summit plateau show that intense internal breakup affects the rigid limestone plate. Since synsedimentary - and tectonic deformation has affected the whole geology of Pletzachkogel and its surroundings, the rockmass has to be considered anisotropic and development of "Hart auf Weich" structures will follow and reactivate these pre-existing tectonic weak zones. Development of radial horizontal stresses by the "Hart auf Weich" process is further amplified by post glacial relaxation of the rockmass.

The anisotropic influence of tectonics is visible when the mapped crack- and depression – orientations of Figure 5-1(a) are compared to the main discontinuity sets of Figure 5-7. Crack set 1 is sub-parallel to fault 1/joint set 1 from Table 4. Since crack set 2 does not clearly correlate with any other observed structure, its origin is seen in in the "Hart auf Weich" process itself.

The big crevasse on the summit plateau can be attributed to the set of tension cracks that develop parallel to the rim of the rigid cover plate, since there is no similar oriented tectonic structure in its proximity. The overall, rugged morphology of the summit plateau is a product of tectonic structures that were reactivated by rock slope deformation. The depression that separated the main summit from the next high point to the north is parallel to joint set 2 and the depression that separates this high point from the next one is parallel to joint set 1/fault 1. Likewise accounts for the col between Pletzachkogel and Sonnwendjoch.

The most impressing morphological feature of Pletzachkogel – the rock buttress in front of the SE cliff face – is not connected with the system "Hart auf Weich". According to Huttenlau and Ortner-Brandstötter (2011), SE-directed normal faults are shaping them. Direct field observation showed that the bedrock between the rock towers is characterized by intense jointing, but no signs of any gravitational or tectonic movement were detected. Concludingly, the shape of the columnar rock buttress was carved out by erosion that attacked deep seated zones of brittle fracturing originating from synsedimentary deformation or alpine tectonics.

Considering the complex interaction of geological framework, glacial processes and gravity, the series of cross sections and therefore the events that shaped the morphology of Pletzachkogel, shall now be discussed:

Step1: sedimentation of HD and PK provided a hard foundation that is covered by a soft layer (KFm) and again overlain by a hard cover (ORK and LJB). Synsedimentary deformation affected the LJB and possibly also ORK which created anisotropic rock mass conditions and introduced primary structural weakness zones.

Step2: NW - directed, fold- and thrust- tectonics during alpine orogenesis have lifted the stratigraphic succession out of the ocean and placed it at today's geographical position and height. Simultaneously, fold axis- and fault parallel zones of weakness were established. The first row of Appendix 4 shows *step1* and *step2*. According to Prager *et al.* (2008) faults and zones of intense brittle fracturing are not only critical for slope stability, but also enable substantial glacial erosion and valley deepening during ice ages which leads to

Step3.: After glacial retreat, the break-shape that defines the morphology of the mountain was carved out. Over steepened cliff faces of ORK and LJB were standing free and unsupported and post-glacial relaxation started to affect the rockmass. In the second row of Appendix 4, distinction is made for two unknown times "t1" and "t2". While time-"t2" at cross section A-A' and C-C' shows the shape of the mountain after the last glacial advance (LGA), time "t1" at cross section B-B' shows the mountains shape after a glaciation, before that (represented by the blue line separating "t1" from "t2"). Patzelt (2012) suggests that the onlap position of moraine onto landslide deposits on the NE side of the mountain, stands for landslide activity on that side of Pletzachkogel prior to the LGA and the other landslides. This conclusion is confirmed by this study's field investigations.

Step4: landslides have occurred on all free sides of Pletzachkogel (i.e. NE, E, S) as a result of the tectonically- and post-glacially amplified "Hart auf Weich" process. While the sliding directions of the landslide at 120-240 AD and the middle Holocene landslide correlate highly with the orientations of joint set 1/fault set 1 and joint set 2 (Table 4), the sliding direction of the late Pleistocene landslide correlates with the identified crack set 2 (Figure 5-1(a)). The inferred morphology of Pletzachkogel at "t1" and "t2" is based on comparison to other mountains in the Inn-valley at the southern rim of the NCA (e.g. Hechenberg, Haller Zuntherkopf). Although also over steepened, close to the Inntal shear zone and suffering from stress redistribution, they did not collapse. This is seen as evidence for the importance of the Kössen Formation as a weak layer in a very unfavorable geometrical position.

7. Conclusion

Compact portable drone platforms for UAV photogrammetry provide an unprecedented ability to capture high resolution 3D georeferenced structural geologic data. Considering the great efficiency with which data can be acquired, UAV–based survey methods are sure to see rapidly increasing deployment, particularly in alpine terrain where site access limitations and personnel safety concerns are significant.

The UAV workflow presented herein has been applied for rock fall source area analysis, and greatly facilitates identification of rock blocks that meet kinematic requirements for a variety of block detachment modes. A key step in the workflow involves extraction of discontinuity orientations from the 3D point cloud. For developing large data sets, efficiency becomes increasingly important, and automated or semi-automated point cloud orientation extraction tools are necessary. The plugins *Facets* and *Compass* developed for the open source software CloudCompare permit automated and semi-automated measurements, respectively, and coincide well with data obtained from manual field measurements. As a result, three different oriented main joint sets were identified, and analyzed concerning potential block failure modes. The data sets obtained are sufficient for performing accurate structural geological analyses of inaccessible areas, and thus can substantially support ground-based geologic field surveys. Furthermore, the identified discontinuities are considered to penetrate the whole mountain and lead to instable rockmass conditions.

The case study of Pletzachkogel shows that stratigraphic and structural geological predispositions can have substantial influence on the geomechanical behavior of a rockmass. The special association of these features produced a mountain where landslides occurred on all free sides, but a multitude of different failure modes and – sizes. Looking for geological features comparable to Pletzachkogel can help with reprocessing of past landslides, or identification of areas prone to them.

The geomechanical system "Hart auf Weich" provides a well-suited model for the explanation of the observed structures and phenomena. Some uncertainties remain however. The structures created by this phenomenon can neither be assigned to tectonics nor to gravitational mass movements and a clear terminology is missing. The original studies and models by Poisel and Eppensteiner were performed with homogeneous - isotropic materials, which is but an abstraction of real rock masses that almost always exhibit anisotropic behavior (see also Barton and Quadros (2015)). More geological and rock mechanical research in these fields is required.

References

Agisoft (2017), “Agisoft PhotoScan”, available at: http://www.agisoft.com/ (accessed 8 October 2017).

Ampferer, O. (1908), “Studien über die Tektonik des Sonnwendgebirges”, *Jahrbuch d. k. k. geol. Reichsanstalt*, Vol. 58 No. 2.

Barton, N. (1976), “The shear strength of rock and rock joints”, *International Journal of Rock Mechanics and Mining Sciences & Geomechanics Abstracts*, Vol. 13 No. 9, pp. 255–279.

Barton, N. and Quadros, E. (2015), “Anisotropy is Everywhere, to See, to Measure, and to Model”, *Rock Mechanics and Rock Engineering*, Vol. 48 No. 4, pp. 1323–1339.

CloudCompare (2017), “CloudCompare”, available at: http://www.cloudcompare.org/ (accessed 8 October 2017).

Czurda, K. (1970), “Das Plattenkalk-Niveau als Übergangsfazies, aufgezeigt am Beispiel der Klostertaler Alpen”, *Verh. Geologische Bundes Anstalt*, pp. 549–550.

Dewez, T.B., Girardeau-Montaut, D., Allanic, C. and Rohmer, J. (2016), “FACETS. A CLOUDCOMPARE PLUGIN TO EXTRACT GEOLOGICAL PLANES FROM UNSTRUCTURED 3D POINT CLOUDS”, *ISPRS - International Archives of the Photogrammetry, Remote Sensing and Spatial Information Sciences*, XLI-B5, pp. 799–804.

DJI (2017), “MAVIC SPECS”, available at: http://www.dji.com/mavic/info#specs (accessed 8 October 2017).

Donofrio, D.A., Brandner, R. and Poleschinski, W. (2003), “Conodonten der Seefled Formation: ein Beitrag zur Bio- und Lithostratigraphie der Hauptdolomit Plattform (Nördliche Kalkalpen, Tirol)”, *Geologische Paläontologische Mitteilungen Innsbruck*, No. 26, pp. 91–107.

Eisbacher, G. and Brandner, R. (1995), “Role of High-Angle Faults during heteroaxial Contraction, Inntal thrust sheet, Norhtern Calcareous Alps, Western Austria”, *Geologische Paläontologische Mitteilungen Innsbruck*, No. 20, pp. 389–406.

Flügel, E. and Stanton, R.J. (1989), “Die Steinplatte (Oberrhätkalk) bei Waidring/Tirol:. Kein Riff Modell”, *Geologische Paläontologische Mitteilungen Innsbruck*, No. 16, pp. 28–29.

Frey, M., Desmons, J. and Neubauer, F. (1999), *The new metamorphic map of the Alps: Introduction*, bis 1977 Leemann / ab 1978 Stäubli.

Fruth, I. and Scherreiks, R. (1982), “Hauptdolomit (Norian) — stratigraphy, paleogeography and diagenesis”, *Sedimentary Geology*, Vol. 32 No. 3, pp. 195–231.

Golas, B. (1996), “Der Eibseebergsturz, Eine geomorphologische Studie”, Dipl. Thesis, Universität Innsbruck, Innsbruck, 1996.

Holstein, B. (2004), “Palynologische Untersuchungen der Kössener Schichten. (Rhät, Alpine Obertrias)”, in *Jahrbuch der geologischen Bundesanstalt*, Wien, pp. 261–365.

Huttenlau, M. and Ortner-Brandstötter, G. (2011), “Risk-based analysis of possible catastrophic rockslide scenarios and linked consequences in Tyrol, Austria”, *Zeitschrift für Geomorphologie, Supplementary Issues*, Vol. 55 No. 3, pp. 179–204.

ORF (2015), “Wege nach Felsstürzen gesperrt”, available at: http://tirol.orf.at/news/stories/2712740/ (accessed 2 July 2017).

Ortner, H. (2017), *Hierlatzkalk*, mündlich.

Ortner, H., Reiter, F. and Brandner, R. (2006), “Kinematics of the Inntal shear zone–sub-Tauern ramp fault system and the interpretation of the TRANSALP seismic section, Eastern Alps, Austria”, *Tectonophysics*, Vol. 414 No. 1-4, pp. 241–258.

Patzelt, G. (2012), “Die Bergstürze vom Pletzachkogel, Kramsach, Tirol”, *Jahrbuch der Geologischen Bundesanstalt*, No. 152, pp. 25–38.

Piller, W., Egger, H., Erharter, C.W., Gross, M., Harzhauser, M., Hubmann, B., van Husen, D., Krenmayr, H.-G., Krystyn, L., Lein, R., Lukender, A., Mandl, G.W., Rögl, F., Roetzel, R., Rupp, C., Schnabel, W., Schönlaub, H., Summesberger, H., Wagreich, M. and Wessely, G. (2004), *Die stratigraphische Tabelle von Österreich 2004: (sedimentäre Schichtfolgen)*.

Poisel, R. and Eppensteiner, W. (1988), “Gang und Gehwerk einer Massenbewegung Teil 1: Geomechanik des Systems >Hart auf Weich<”, *Felsbau*, No. 6, pp. 189–194.

Poisel, R. and Eppensteiner, W. (1989), “Gang und Gehwerk einer Massenbewegung Teil 2: Massenbewegungen am Rand des Systems >Hart auf Weich<”, *Felsbau*, No. 7, pp. 16–20.

Prager, C., Zangerl, C., Patzelt, G. and Brandner, R. (2008), “Age distribution of fossil landslides in the Tyrol (Austria) and its surrounding areas”, *Natural Hazards and Earth System Science*, Vol. 8 No. 2, pp. 377–407.

Resch, W., Sarntheim, M., Allert, T. and Tiedemann, R.B. (1986), “Zum Gosaurelief am Pletzachkogel im südöstlichen Rofangebirge (Nördliche Kalkalpen, Tirol)”, *Mitteilungen der Bayerischen Staatssammlung für Paläontologie und Histor. Geologie*, No. 26, pp. 113–120.

Schmid, S.M., Fuegenschuh, B., Kissling, E. and Schuster, R. (2004), "Tectonic map and overall architecture of the Alpine orogen", *Eclogae Geologicae Helvetiae*, Vol. 97 No. 1, pp. 93–117.

Thiele, S.T., Grose, L., Samsu, A., Micklethwaite, S., Vollgger, S.A. and Cruden, A.R. (2017), "Rapid, semi-automatic fracture and contact mapping for point clouds, images and geophysical data", *Solid Earth Discussions*, pp. 1–19.

tiris (2017), "Tiroler Rauminformationssystem", available at: https://www.tirol.gv.at/statistik-budget/tiris/ (accessed 30 November 2017).

Vörös, A. (1991), "Hierlatzkalk - a Peculiar Austro Hungarian Jurassic Facies", in Lobitzer, H. and Császár, G. (Eds.), *Jubiläumsschrift 20 Jahre geologische Zusammenarbeit Österreich-Ungarn*, Geologische Bundesanstalt, Wien.

Wagreich, M. and Faupl, P. (1994), "Palaeogeography and geodynamic evolution of the Gosau Group of the Northern Calcareous Alps (Late Cretaceous, Eastern Alps, Austria)", *Palaeogeography, Palaeoclimatology, Palaeoecology*, Vol. 110 No. 3-4, pp. 235–254.

Waltham, T. (2002), "The engineering classification of karst with respect to the role and influence of caves", *International Journal of Speleology*, No. 31, pp. 19–35.

Wyllie, D.C., Mah, C.W. and Hoek, E. (2004), *Rock slope engineering: Civil and mining,* 4th ed., Spon Press, London, New York.

Appendix:

Appendix 1; Coordinates of the ground control points given in MGI / Austria GK West (EPSG: 31254). Note that point c1f and c2a share the same coordinates.

Chunk	Name	Easting	Northing	Height	KQ-Lage	KQ-Höhe
1	c1a	114174.503	258042.717	1093.518	0.010	0.023
1	c1b	114145.741	258054.333	1115.881	0.007	0.019
1	c1c	114137.352	258066.992	1127.118	0.007	0.019
1	c1d	114127.504	258081.476	1139.800	0.011	0.028
1	c1e	114125.032	258103.653	1156.211	0.014	0.032
1	c1f	114119.583	258129.630	1176.474	0.015	0.030
2	c2a	114119.583	258129.630	1176.474	0.015	0.030
2	c2b	114108.779	258089.002	1150.376	0.008	0.022
2	c2c	114085.852	258076.106	1154.849	0.009	0.018
2	c2d	114061.427	258091.066	1176.145	0.008	0.013
2	c2e	114041.035	258120.388	1204.203	0.012	0.018
2	c2f	114037.389	258154.930	1228.058	0.013	0.021
3	c3a	113941.853	258109.436	1207.096	0.013	0.015
3	c3b	113946.919	258127.000	1217.793	0.015	0.018
3	c3c	113972.328	258138.358	1222.636	0.014	0.020
3	c3d	113979.747	258129.422	1211.788	0.013	0.019
3	c3e	114010.261	258151.703	1230.215	0.014	0.018
3	c3f	114018.477	258179.46	1247.540	0.015	0.016

Appendix 2; Agisoft PhotoScan processing- and point cloud parameters

	chunk1	chunk2	chunk3
General			
Aligned cameras	426	389	592
Estimated image quality	0.84-0.90	0.76-0.9	0.81-0.88
Markers	6	6	6
Coordinate system	MGI/Austria GK West	MGI/Austria GK West	MGI/Austria GK West
Sparse Point Cloud			
Points	98,438	83,321	91,432
RMS reprojection error	0.282003 (1.11413 pix)	0.279052 (1.22733 pix)	0.315064 (1.68384 pix)
Max reprojection error	3.75983 (44.2923 pix)	9.24692 (36.4791 pix)	5.71909 (40.5978 pix)
Mean key point size	3.67289 pix	4.02572 pix	5.17365 pix
Effective overlap	9.31004	8.71713	10.2095
Alignment parameters			
Accuracy	High	High	High
Pair preselection	Disabled	Disabled	Generic
Key point limit	40,000	40,000	40,000
Tie point limit	10,000	10,000	10,000
Constrain features by mask	Yes	Yes	Yes
Adaptive camera model fitting	Yes	Yes	Yes
Matching time	8 hours 41 minutes	6 hours 38 minutes	2 hours 45 minutes
Alignment time	23 minutes 33 seconds	18 minutes 52 seconds	55 minutes 4 seconds
Optimization parameters			
Parameters	f, b1, b2, cx, cy, k1-k4, p1, p2	f, b1, b2, cx, cy, k1-k4, p1, p2	f, b1, b2, cx, cy, k1-k4, p1, p2
Optimization time	7 seconds	6 seconds	8 seconds
Depth Maps			
Count	410	386	494

Reconstruction parameters			
Quality	High	High	High
Filtering mode	Aggressive	Aggressive	Aggressive
Processing time	4 hours 42 minutes	4 hours 17 minutes	3 hours 28 minutes
Dense Point Cloud			
Points	41,805,462	49,762,919	42,481,210
Reconstruction parameters			
Quality	High	High	High
Depth filtering	Aggressive	Aggressive	Aggressive
Depth maps generation time	4 hours 42 minutes	4 hours 17 minutes	3 hours 28 minutes
Dense cloud generation time	2 days 2 hours	1 days 5 hours	3 days 3 hours
Model			
Faces	8,361,017	9,952,448	8,496,241
Vertices	4,189,819	4,986,992	4,256,137
Texture	8,192 x 8,192, uint8	8,192 x 8,192, uint8	8,192 x 8,192, uint8
Reconstruction parameters			
Surface type	Arbitrary	Arbitrary	Arbitrary
Source data	Dense	Dense	Dense
Interpolation	Enabled	Enabled	Enabled
Quality	High	High	High
Depth filtering	Aggressive	Aggressive	Aggressive
Face count	8,361,017	9,952,449	8,496,242
Processing time	34 minutes 9 seconds	40 minutes 42 seconds	1 hours 9 minutes
Texturing Parameters			
Mapping mode	Generic	Generic	Generic
Blending mode	Mosaic	Mosaic	Mosaic
Texture size	8,192 x 8,192	8,192 x 8,192	8,192 x 8,192
Enable color correction	No	No	No
Enable hole filling	Yes	Yes	Yes
UV mapping time	2 minutes 14 seconds	2 minutes 3 seconds	1 minutes 54 seconds
Blending time	5 minutes 31 seconds	5 minutes 46 seconds	5 minutes 49 seconds

Appendix 3; Placeholder for Geological Map

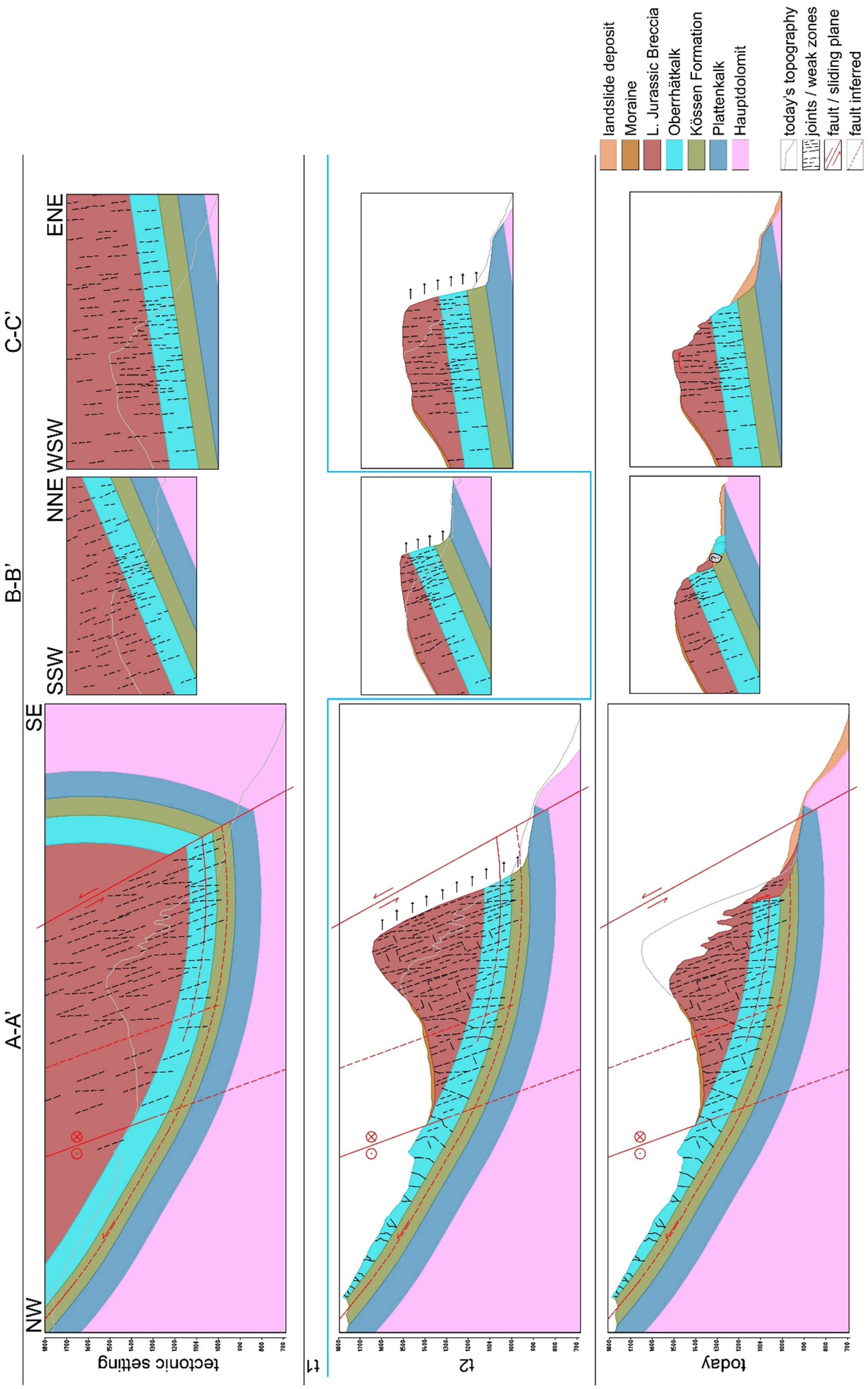

Appendix 4; Cross sections based on the geological map. Top row: tectonic setting of Pletzachkogel. Bottom row: today's geology. Middle row: situation before failure of the mountain flanks. The blue line which separates "t1" from "t2", represents the last glacial advance.